

Chlorophyll biomass in the global oceans: satellite retrieval using inherent optical properties

Paul E. Lyon, Frank E. Hoge, C. Wayne Wright, Robert N. Swift, and James K. Yungel

In the upper layer of the global ocean, 2082 *in situ* chlorophyll biomass values $\langle \text{Chl} \rangle$ are retrieved by concurrent satellite-derived inherent optical properties (IOP). It is found that (1) the phytoplankton absorption coefficient IOP alone does not provide satisfactory $\langle \text{Chl} \rangle$ retrieval; (2) the chromophoric dissolved organic matter (CDOM) absorption coefficient IOP must also be used to obtain satisfactory retrieval through $\langle \text{Chl} \rangle \propto a_{\text{ph}} + pa_{\text{CDOM}}$ where p is a constant and a_{ph} and a_{CDOM} are, respectively, the phytoplankton and CDOM absorption coefficients; (3) the IOP-based $\langle \text{Chl} \rangle$ retrieval performance is comparable to standard satellite reflectance ratio retrievals (that have CDOM absorption intrinsically embedded within them); (4) inclusion of the total backscattering coefficient IOP does not contribute significantly to $\langle \text{Chl} \rangle$ retrieval; and (5) the new IOP-based algorithm may provide the possibility for future research to establish the actual role of extracellular CDOM from all sources in the intracellular production of chlorophyll biomass. © 2004 Optical Society of America

OCIS codes: 010.4450, 280.0280, 300.6550.

1. Introduction

Historically, satellite retrieval of chlorophyll biomass $\langle \text{Chl} \rangle$ utilizes reflectance ratio algorithms.^{1,2} These reflectance ratios strongly suggest that chlorophyll biomass is related to oceanic absorption inherent optical properties (IOPs). Also, independent field measurements have shown that reflectance ratios are correlated with the sum of the phytoplankton and chromophoric dissolved organic matter (CDOM) absorption coefficients³ ($a_{\text{ph}} + a_{\text{CDOM}}$).

More recently, radiative transfer inversions have provided chlorophyll retrievals concurrently with some IOPs.^{4–6} However, the relationship of the principal IOPs, a_{ph} and a_{CDOM} , to $\langle \text{Chl} \rangle$ variability is not clearly revealed in these studies.

The purpose of this paper is to suggest that (1) IOP versus $\langle \text{Chl} \rangle$ relationships can be used to retrieve the chlorophyll biomass and (2) there is a more direct bio-optical link between absorption IOPs and chlorophyll biomass.

2. Theory

First, the historical laboratory correlation of the phytoplankton absorption coefficient versus $\langle \text{Chl} \rangle$ is briefly reviewed to establish the usual operative equation $a_{\text{ph}} = A\langle \text{Chl} \rangle^B$ or $\langle \text{Chl} \rangle = (a_{\text{ph}}/A)^{1/B}$. Second, the connection among $\langle \text{Chl} \rangle$, reflectance ratios, and oceanic absorption IOPs (a_{ph} and a_{CDOM}) is reviewed and established by both radiative transfer and corroborative field experimental findings. Third, the operative laboratory equation $\langle \text{Chl} \rangle = (a_{\text{ph}}/A)^{1/B}$ is generalized to include the a_{CDOM} IOP. Finally, the exponential formulation of the IOP-based $\langle \text{Chl} \rangle$ retrieval relationship is established.

A. Laboratory Retrieval of Chlorophyll Biomass

Experimentally it is found by laboratory measurements of a_{ph} and extracted chlorophyll pigment biomass that

$$a_{\text{ph}} \propto \langle \text{Chl} \rangle. \quad (1)$$

Operationally,

$$a_{\text{ph}} \equiv \alpha^* \langle \text{Chl} \rangle, \quad (2)$$

where α^* is the chlorophyll-specific absorption coefficient (that varies widely depending on light history, nutrient availability, and species).

Copious laboratory measurements yield a more robust relationship⁷:

$$a_{\text{ph}} \equiv A \langle \text{Chl} \rangle^B, \quad (3)$$

The authors are with Wallops Flight Facility, Wallops Island, Virginia 23337: P. E. Lyon, R. N. Swift, and J. K. Yungel, EG&G Incorporated; F. E. Hoge (frank.hoge@nasa.gov) and C. W. Wright, NASA, Goddard Space Flight Center.

Received 19 December 2003; revised manuscript received 15 June 2004; accepted 19 August 2004.

0003-6935/04/315886-07\$15.00/0

© 2004 Optical Society of America

which essentially reduces to Eq. (2) when $B = 1$. For laboratory retrievals Eq. (3) yields

$$\langle \text{Chl} \rangle = \left(\frac{a_{\text{ph}}}{A} \right)^{\frac{1}{B}}, \quad (4)$$

where A and B also vary widely depending on light history, nutrient availability, and species. Of course chlorophyll biomass variability induced by the other principal oceanic IOPs (the CDOM absorption coefficient) is not available through this type of laboratory analysis.

B. Oceanic Retrieval of Chlorophyll Biomass

The satellite retrieval of chlorophyll biomass in the real oceanic environment is considerably more complex than laboratory filter pad absorption measurements of a_{ph} and the corresponding chlorophyll biomass extractions. Specifically, it can be shown that $\langle \text{Chl} \rangle \sim a$ (the total absorption), and this is the fundamental basis of the algorithm derived here. This is achieved through simple radiative transfer theory and field experiments.

First, for many years it has been shown that chlorophyll biomass is related to water-leaving reflectance ratios^{1,2} or

$$\langle \text{Chl} \rangle \propto \text{reflectance ratios}. \quad (5)$$

The reflectance ratio chlorophyll algorithm is essentially a total absorption algorithm. This can be easily shown when we recall that at 443 nm (the approximate absorption peak of chlorophyll pigment) the reflectance R is roughly approximated by $R_{\text{rs}}(443) = \text{constant} \times b_b(443)/a(443)$; and at the lower chlorophyll absorption hinge point, $R_{\text{rs}}(555) = \text{constant} \times b_b(555)/a(555)$ where b_b is the total backscattering coefficient and a is again the total absorption coefficient. Thus a reflectance ratio can be formed: $R_{\text{rs}}(555)/R_{\text{rs}}(443) \sim \text{constant} \times b_b(555)/b_b(443)a(443)/a(555)$. It is subsequently found that backscattering has little influence on the $\langle \text{Chl} \rangle$ variability, but at this point in the derivation the backscattering ratio $b_b(555)/b_b(443)$ is assumed to have modest variation. Thus $R_{\text{rs}}(555)/R_{\text{rs}}(443) \sim \text{constant} \times a(443)/a(555)$. Then, because IOPs can be rigorously summed,

$$\langle \text{Chl} \rangle \sim \text{constant} \times \frac{a_{\text{water}}(443) + a_{\text{ph}}(443) + a_{\text{CDOM}}(443)}{a_{\text{water}}(555) + a_{\text{ph}}(555) + a_{\text{CDOM}}(555)}.$$

The reflectance ratio can be expressed entirely in terms of the absorption at a reference wavelength. Using 443 nm as the reference wavelength, we obtain $a_{\text{water}}(555) = C_1 a_{\text{water}}(443)$ and $a_{\text{ph}}(555) \approx$

$C_2 a_{\text{ph}}(443)$ (Ref. 8); for a CDOM spectral slope of $\sim 0.017/\text{nm}$, $a_{\text{CDOM}}(555) \approx 0.15 a_{\text{CDOM}}(443)$, yielding

$$\langle \text{Chl} \rangle \sim \text{constant} \times \frac{a_{\text{water}}(443) + a_{\text{ph}}(443) + a(443)_{\text{CDOM}}}{C_1 a_{\text{water}}(443) + C_2 a_{\text{ph}}(443) + 0.15 a(443)_{\text{CDOM}}}.$$

In this paper descriptive constants (having unspecified values) are given by C_i where $i = 1, 2, 3, \dots$. Because a_{water} is constant, this suggests that the variability of the reflectance ratio (or chlorophyll) is strongly driven by $a_{\text{ph}}(443)$ and $a_{\text{CDOM}}(443)$.

Thus the general application of relation (5) yields

$$\langle \text{Chl} \rangle \propto a_{\text{ph}} + a_{\text{CDOM}}. \quad (6)$$

Second, in the oceanic environment an important finding was recently revealed by field experiments: Water-leaving reflectance ratios are strongly related to the sum of the phytoplankton absorption and the CDOM absorption³ (see especially Fig. 12 in Ref. 3), or

$$\text{reflectance ratios} \propto a_{\text{ph}} + a_{\text{CDOM}}. \quad (7)$$

Thus, using relation (5) for oceanic field measurement of IOPs and reflectances, we obtain $\langle \text{Chl} \rangle \propto a_{\text{ph}} + a_{\text{CDOM}}$ as given in relation (6).

Without using reflectance ratios, but in analogy to laboratory determinations, we can give a general form of oceanic *in situ* chlorophyll biomass retrieval using only the a_{ph} and a_{CDOM} IOPs:

$$\langle \text{Chl} \rangle = \left(\frac{A_1 a_{\text{ph}} + A_2 a_{\text{CDOM}}}{A_3} \right)^{\frac{1}{B}}. \quad (8)$$

Inside the parentheses we define $A_3/A_1 \equiv A$ and $A_2/A_1 \equiv p$ where A , B , and p are algorithm constants to be determined. Then

$$\langle \text{Chl} \rangle = \left(\frac{a_{\text{ph}} + p a_{\text{CDOM}}}{A} \right)^{\frac{1}{B}}. \quad (9)$$

In log space, this is a linear relationship:

$$\ln(\langle \text{Chl} \rangle) = \frac{1}{B} \ln(a_{\text{ph}} + p a_{\text{CDOM}}) + \frac{\ln(A)}{B}. \quad (10)$$

Preliminary analysis of $\langle \text{Chl} \rangle$ has shown that Eq. (10) gives a reasonable fit to the *in situ* data and $(a_{\text{ph}} + p a_{\text{CDOM}})$ ($r_{\text{linear}}^2 = 0.279$, $r_{\text{log}}^2 = 0.810$). However, an order 5 polynomial yields a notably better agreement between $\langle \text{Chl} \rangle$ and $(a_{\text{ph}} + p a_{\text{CDOM}})$ in regions of high total absorption ($r_{\text{linear}}^2 = 0.371$, $r_{\text{log}}^2 = 0.813$). Thus we formulate the IOP-based chlorophyll biomass algorithm as

$$\langle \text{Chl} \rangle = \exp(q_5 x^5 + q_4 x^4 + q_3 x^3 + q_2 x^2 + q_1 x + q_0), \quad (11)$$

where

$$x \equiv \ln[a_{\text{ph}} + p(a_{\text{CDOM}})^{1/2}]. \quad (12)$$

Here the q_i 's and p are determined by least-squares methods described below. Note that the chlorophyll biomass given by Eq. (11) is empirical, just like the standard OC4v4 algorithm; it is not based on reflectance ratios but is explicitly linked to IOPs within the polynomial. The $a_{ph}(\lambda)$ and $a_{CDOM}(\lambda)$ IOPs are obtained by linear matrix inversion of a radiative transfer model.⁹⁻¹⁴ The CDOM model slope was held fixed at 0.018/nm, but the backscattering wavelength ratio model exponent variability is propagated into the CDOM absorption coefficient.^{9,11} For $a_{ph}(\lambda)$ and $a_{CDOM}(\lambda)$ IOPs at $\lambda = 412$ nm, the values of the parameters are given in Table 1. (Note that any of the wavelengths used in the linear matrix inversion, 412, 490, and 555 nm, can be used because the IOP

Table 1. Algorithm Constants $q_0, q_1, q_2, q_3, q_4, q_5,$ and p at 412 nm for Eqs. (11) and (12)

λ	q_0	q_1	q_2	q_3	q_4	q_5	p
412 nm	2.7702	0.9457	0.8765	0.9038	0.2598	0.025	0.016

models are valid at these wavelengths, although separate q_i 's and the p coefficient must be derived for each wavelength used.⁹⁻¹³ The square root applied to the $a_{CDOM}(\lambda)$ coefficient magnifies the effect of the $a_{CDOM}(\lambda)$ on x when $a_{CDOM}(\lambda)$ is <1.0 (1/m) and lowers its effect when $a_{CDOM}(\lambda)$ is >1.0 (1/m). The inclusion of the square root is purely a tool to improve

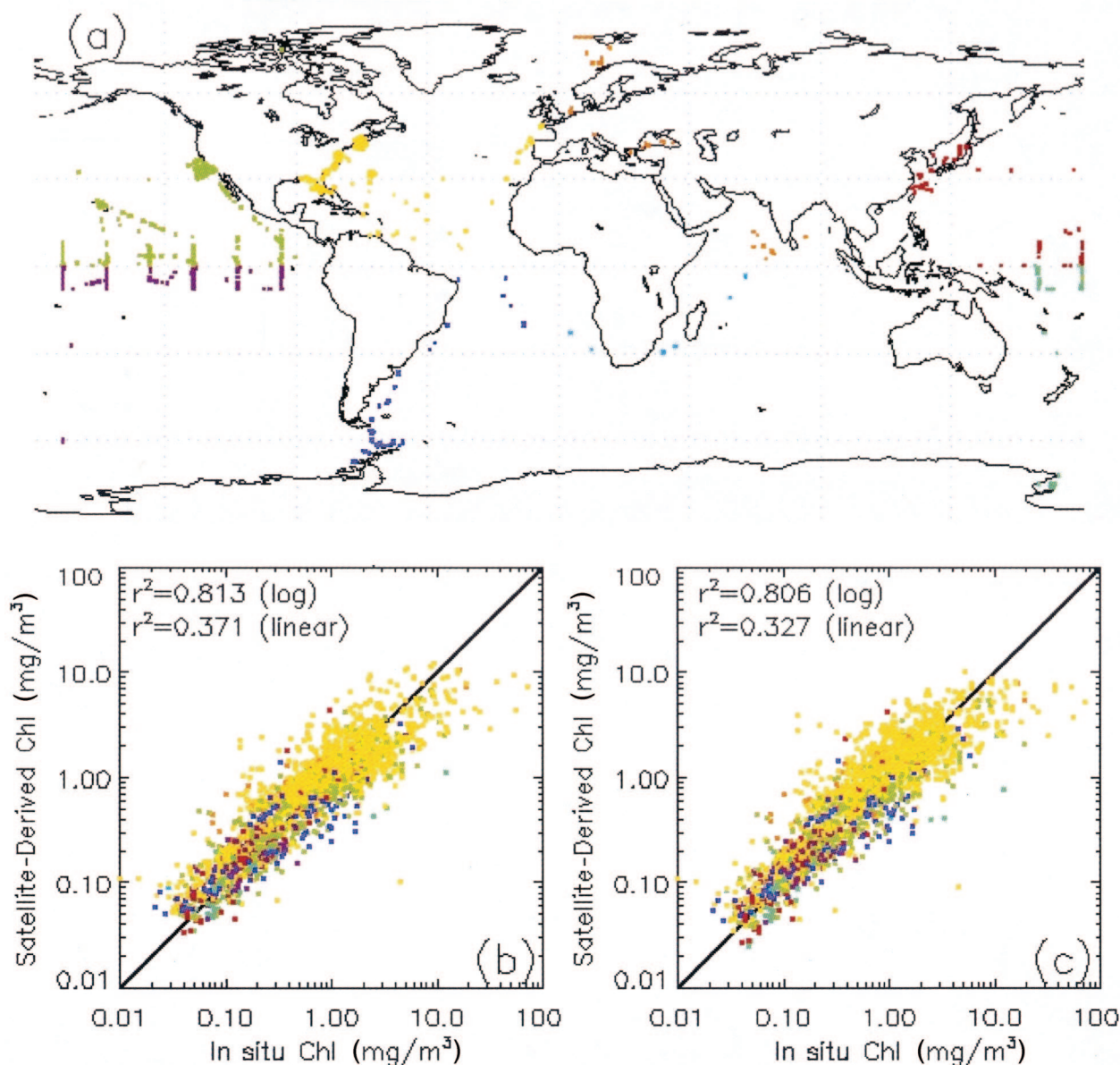


Fig. 1. (a) Global distribution of the $N = 2082$ *in situ* chlorophyll biomass values, color coded into eight regions. (b) Retrieval of the 2082 *in situ* chlorophyll [$\text{Chl} = f(a_{ph}, a_{CDOM})$] by the IOP-based method given in Eqs. (11) and (12). (c) Retrieval of the 2082 *in situ* chlorophyll values with the standard SeaWiFS OC4v4 algorithm. Comparison of the correlation coefficients in (b) and (c) shows that the absorption IOP-based retrievals and the SeaWiFS standard OC4v4 algorithmic retrievals are quite comparable.

the performance of the IOP-based empirical algorithm. [We found that the backscattering coefficient contribution was not significant and could be excluded from Eq. (12) and is therefore not included in the final formulation of the algorithm. The backscattering coefficient contribution is further discussed in Section 3 in concert with an illustration of the variability separately contributed by each IOP.] Equations (11) and (12) are valid for any sensor, either active or passive, that concurrently provides a_{ph} and a_{CDOM} .

We derived the q_i coefficients used in Eq. (11) by varying p in Eq. (12) through a range from 0.0 to 2.0 and solving the least-squares fit of Eq. (11) to the *in situ* chlorophyll data to derive the q 's associated with each value of p . A correlation coefficient was calculated between the $\langle \text{Chl} \rangle$ derived from the empirical algorithm and the *in situ* $\langle \text{Chl} \rangle$ data for each set of coefficients. The set of p and q_i 's that gave the highest correlation coefficient was used in the final version of the algorithm.

3. Results

Sea-Viewing Wide Field-of-View Sensor (SeaWiFS) global area coverage data were processed through IOP inversion and global binning routines to derive daily global maps of IOPs.¹³ We obtained the biomass values from the Goddard Space Flight Center's SeaWiFS and Sensor Intercomparison and Merger for Biological and Interdisciplinary Oceanic Studies (SIMBIOS) archive by retaining only those values within the upper 5 m of the surface layer. The *in situ* $\langle \text{Chl} \rangle$ data set was compared with the daily global IOP maps, and a match-up data set was created with only *in situ* $\langle \text{Chl} \rangle$ values that were obtained within 24 h of the SeaWiFS IOP data points. We then modified this match-up data set by averaging all *in situ* $\langle \text{Chl} \rangle$ data that were coincident with a single bin within a daily global map. There were 29,992 *in situ* $\langle \text{Chl} \rangle$ data points in the original data set, and 6549 of those values were coincident with SeaWiFS overpasses. The cleaning process that averaged all $\langle \text{Chl} \rangle$ values within a single bin for a given day reduced the number of match-up values to 2127. We then reduced the match-up data set to 2082 data points by excluding any satellite data that had either $a_{ph}(412 \text{ nm}) > 1.0$ (1/m) or $a_{CDOM}(412 \text{ nm}) > 1.0$ (1/m) as determined by model inversion of the SeaWiFS reflectances. Water masses with IOP values in this range generally cause problems for both the IOP inversion process and the atmospheric correction procedures applied to the SeaWiFS R_{rs} values.

Figure 1(a) shows the global distribution of the 2082 *in situ* chlorophyll biomass values, color coded into eight regions. Figure 1(b) shows retrieval of the 2082 *in situ* values by use of the IOP-based method given by Eqs. (11) and (12). Figure 1(c) shows retrieval of the 2082 *in situ* values by use of the standard SeaWiFS OC4v4 algorithm. (The 1:1 lines provided in Fig. 1 and in Figs. 2–4 are a visual aid; and to improve clarity, the computed regression lines are not illustrated.) Comparison of the correlation

coefficients shows that the absorption IOP-based retrievals and the SeaWiFS standard OC4v4 algorithmic retrievals are quite comparable. (Because satellite IOP retrievals and the resulting IOP-based chlorophyll algorithms are relatively recent developments, it is reasonable to expect that IOP-based chlorophyll algorithm performance will eventually surpass that of reflectance ratio algorithms.) The color-coded pixels in the scatter plots in Figs. 1(b) and 1(c) show that the algorithms do not seem to be biased in any region. The substantial agreement of the IOP-based algorithm and the standard SeaWiFS algorithm is also demonstrated in the scatter plot of the IOP-based versus OC4v4 retrievals given in Fig. 2.

However, there is an important advantage to the IOP-based retrieval: It allows for the study of the variation of the chlorophyll biomass as a function of the absorption coefficients of phytoplankton and extracellular CDOM (see Fig. 3). In Fig. 3 it can be seen that the chlorophyll biomass increases rather rapidly for smaller values of the absorption coefficients of both phytoplankton and CDOM. The increasing influence of the phytoplankton absorption coefficient is especially strong up to a barely perceptible plateau at $\sim 0.3/\text{m}$, at which point its influence diminishes. Compared with phytoplankton absorption, the CDOM absorption influence is somewhat similar but varies more smoothly and shows no obvious plateau. It has been shown¹⁵ that the phytoplankton absorption coefficient IOP provides a better retrieval of primary production than chlorophyll biomass. Figure 3 provides possible interpretive evidence: The phytoplankton are photoacclimating to the varying CDOM absorption, i.e., increasing CDOM absorption leads to reduced irradiance incident upon

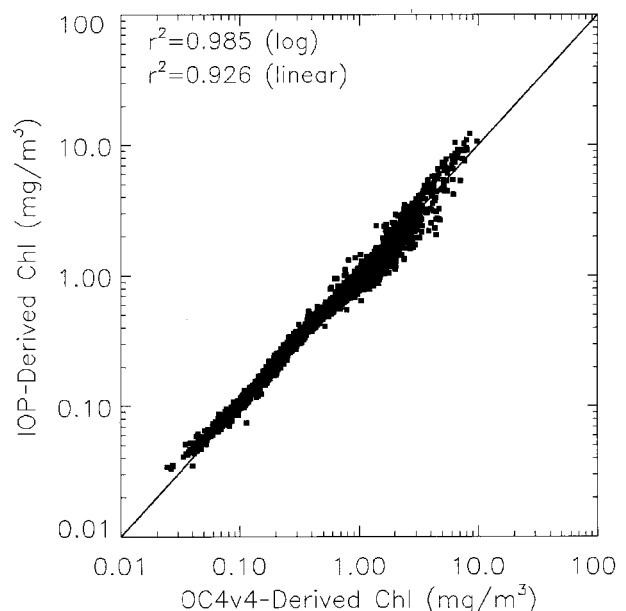


Fig. 2. Scatter plot of IOP-based retrievals versus standard SeaWiFS OC4v4 retrievals [OC4v4 versus $f(a_{ph}, a_{CDOM})$] for 2082 *in situ* chlorophyll values in Fig. 1 showing substantial agreement for the two algorithms.

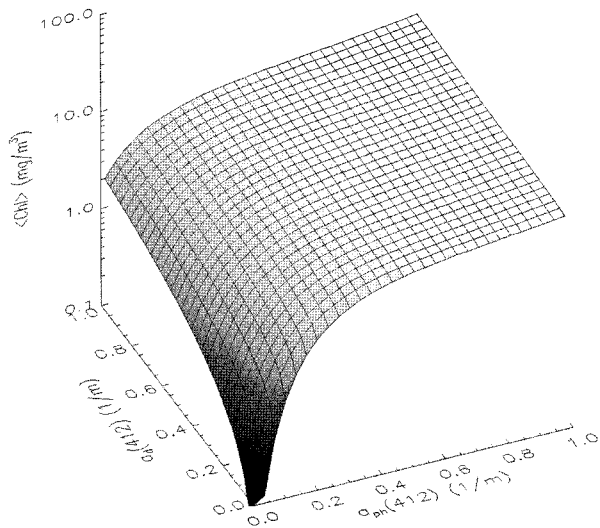


Fig. 3. Phytoplankton and CDOM absorption-induced chlorophyll biomass variability generated by use of the IOP-based algorithm in Eqs. (11) and (12).

the phytoplankton whose response is then to produce increasing amounts of chlorophyll (and vice versa).

Figures 4(a)–4(d) illustrate the correlation of the *in situ* chlorophyll biomass with each SeaWiFS-retrieved IOP: total constituent backscattering coefficient, phytoplankton absorption coefficient, CDOM absorption coefficient, and both phytoplankton and CDOM absorption coefficients combined as in Eqs. (11) and (12). The IOPs in Figs. 4(a)–4(c) were regressed to the *in situ* chlorophyll with Eq. (4). In Fig. 4(a) the constituent backscattering is weakly but positively correlated with *in situ* chlorophyll biomass. Recall that the constituent backscattering is not used within the chlorophyll biomass IOP-based retrieval algorithm because it contributed no noticeable improvement. The correlations of the *in situ* chlorophyll biomass with the phytoplankton absorption coefficient IOP [Fig. 4(b)] and with the CDOM absorption coefficient [Fig. 4(c)] are both higher than the constituent backscattering but not remarkably so. [Note that for Figs. 4(a)–4(c), Eq. (4) was essentially used and best fit for each IOP.] However,

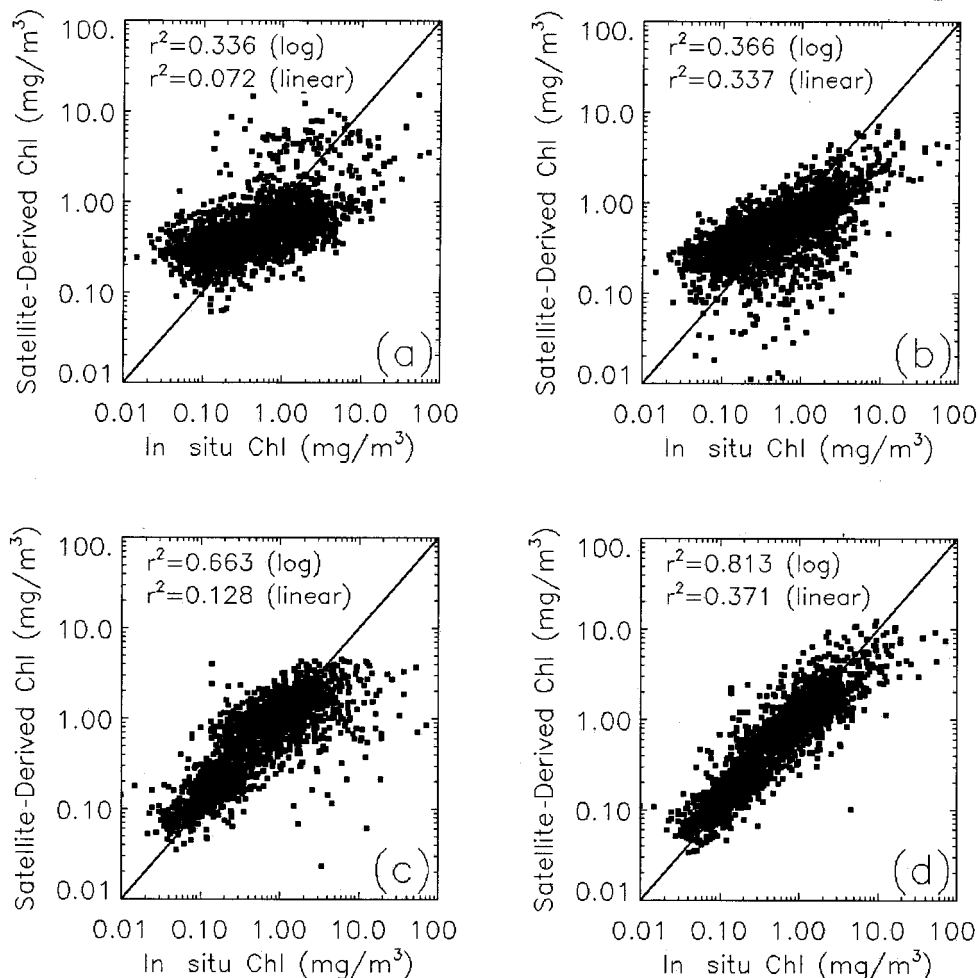


Fig. 4. Correlation of *in situ* chlorophyll biomass versus SeaWiFS-retrieved IOPs: (a) total constituent backscattering coefficient [$\langle \text{Chl} \rangle = f(b_{\text{bt}})$], (b) phytoplankton absorption coefficient [$\langle \text{Chl} \rangle = f(a_{\text{ph}})$], (c) CDOM absorption coefficient, [$\langle \text{Chl} \rangle = f(a_{\text{CDOM}})$], (d) both phytoplankton and CDOM absorption coefficients [$\langle \text{Chl} \rangle = f(a_{\text{ph}}, a_{\text{CDOM}})$] combined as in Eqs. (11) and (12). The latter IOP-based chlorophyll retrievals compare favorably with the empirical SeaWiFS OC4v4 chlorophyll biomass algorithm as shown in Figs. 1(b) and 1(c).

when used in combination [see Eqs. (11) and (12)], the phytoplankton and CDOM absorption coefficients produce a notable correlation with the *in situ* chlorophyll biomass [Fig. 4(d)] [and compares favorably with the SeaWiFS chlorophyll biomass as shown above and discussed relative to Figs. 1(b) and 1(c)].

4. Summary and Discussion

On the basis of historical reflectance ratios, recent ship cruise findings,³ and radiative transfer theory, a new absorption-based chlorophyll biomass algorithm is derived. When used to retrieve 2082 *in situ* global chlorophyll biomass values, the IOP-based algorithm [Eqs. (11) and (12)] is found to be comparable in performance to the standard SeaWiFS OC4v4 chlorophyll biomass algorithm. However, unlike reflectance ratio algorithms, the new IOP-based algorithm allows studies of chlorophyll biomass variability as a function of phytoplankton and CDOM absorption. For example, the chlorophyll surface (Fig. 3) shows significant biomass variability for small amounts of phytoplankton and CDOM absorption.

For chlorophyll biomass variability, the exact role of CDOM absorption is not yet understood but it is hypothesized here to be related to phytoplankton photoacclimation, i.e., the increased absorption of CDOM leads to decreased light availability and in turn the phytoplankton produce more chlorophyll in response. For example, as supporting evidence, the IOP-based algorithm here has an exponential form that is similar to the photoacclimation form,¹⁶ i.e., it has been shown¹⁶ that, for 342 observations related to 23 phytoplankton species,

$$\langle \text{Chl}_{\text{norm}} \rangle = 0.036 + 0.3 \exp(-1.1 I_g).$$

Here $\langle \text{Chl}_{\text{norm}} \rangle$ is a normalized cellular chlorophyll biomass and I_g is the growth irradiance (in mol quanta $\text{m}^{-2} \text{h}^{-1}$), i.e., the cellular chlorophyll declines exponentially with increasing growth irradiance. Note that a specific growth irradiance wavelength is unspecified in the theory given in Ref. 16. For satellite remote sensing purposes, one can attempt to capture the above laboratory-derived exponential variation by assuming that the *in situ* oceanic photoacclimation-induced chlorophyll biomass $\langle \text{Chl} \rangle_{\text{oceanic photoacc}}$ is given by

$$\langle \text{Chl} \rangle_{\text{oceanic photoacc}} \sim \exp[-sE_d(Z)], \quad (13)$$

where $E_d(Z)$ (in $\text{W m}^{-2} \text{nm}^{-1}$) is the plane irradiance at depth Z and serves as a reasonable surrogate for the laboratory growth irradiance. Here s is defined as the slope of irradiance versus chlorophyll photoacclimation within an oceanic province. Prior research¹⁶ strongly suggests that s is species dependent, but for satellite remote sensing purposes s must initially be considered to be a single global species average. But at any depth, $E_d(Z) = E_d(0^-) \exp(-K_d Z)$ where $E_d(0^-)$ is the downwelling irradiance just beneath the ocean surface. The IOPs enter by $K_d \approx (a + b_b)/\mu$ where $a = a_w + a_{\text{ph}} + a_{\text{CDOM}}$, b_b is the total backscattering, and μ is the

average cosine of the downwelling light field. As with Eq. (11), the photoacclimation hypothesis given by Eq. (13) also suggests that IOPs play a strong role in the chlorophyll variability in the global oceans. Additional modeling and analysis studies, outside the scope of this paper, are required to demonstrate equivalence, if any, of the IOP-based chlorophyll retrieved by Eq. (11) and the photoacclimation-induced chlorophyll biomass variability as given by Eq. (13).

References

1. J. E. O'Reilly, S. Maritorena, B. G. Mitchell, D. A. Siegel, K. L. Carder, S. A. Garver, M. Kahru, and C. McClain, "Ocean color chlorophyll algorithms for SeaWiFS," *J. Geophys. Res.* **103**, 24937–24953 (1998).
2. H. R. Gordon, D. K. Clark, J. W. Brown, O. B. Brown, R. H. Evans, and W. W. Broenkow, "Phytoplankton pigment concentrations in the Middle Atlantic Bight: comparison between ship determinations and the coastal zone color scanner estimates," *Appl. Opt.* **22**, 20–36 (1983).
3. M. D. DeGrandpre, A. Vodacek, R. K. Nelson, E. J. Bruce, and N. V. Blough, "Seasonal seawater properties of the U.S. Middle Atlantic Bight," *J. Geophys. Res.* **101**, 22727–22736 (1996).
4. S. A. Garver and D. A. Siegel, "Inherent optical property inversion of ocean spectra and its biogeochemical interpretation. 1. Time series from the Sargasso Sea," *J. Geophys. Res.* **102**, 18607–18625 (1997).
5. K. L. Carder, F. R. Chen, Z. P. Lee, S. K. Hawes, and D. Kamykowski, "Semianalytic Moderate-Resolution Imaging Spectrometer algorithms for chlorophyll *a* and absorption with bio-optical domains based on nitrate-depletion temperatures," *J. Geophys. Res. (Oceans)* **104**, 5403–5421 (1999).
6. R. M. Chomko, H. R. Gordon, S. Maritorena, and D. A. Siegel, "Simultaneous retrieval of oceanic and atmospheric parameters for ocean color imagery by spectral optimization: a validation," *Remote Sens. Environ.* **84**, 208–220 (2003).
7. A. Bricaud, M. Babin, A. Morel, and H. Claustre, "Variability in the chlorophyll-specific absorption coefficients of natural phytoplankton: analysis and parameterization," *J. Geophys. Res.* **100**, 13321–13332 (1995).
8. N. Hoepffner and S. Sathyendranath, "Determination of the major groups of phytoplankton pigments from the absorption spectra of total particulate matter," *J. Geophys. Res.* **98**, 22789–22803 (1993).
9. F. E. Hoge and P. E. Lyon, "Satellite retrieval of inherent optical properties by linear matrix inversion of oceanic radiance models: an analysis of model and radiance measurement errors," *J. Geophys. Res.* **101**, 16631–16648 (1996).
10. F. E. Hoge, C. W. Wright, P. E. Lyon, R. N. Swift, and J. K. Yungel, "Satellite retrieval of the absorption coefficient of phytoplankton phycoerythrin pigment: theory and feasibility status," *Appl. Opt.* **38**, 7431–7441 (1999).
11. F. E. Hoge, C. W. Wright, P. E. Lyon, R. N. Swift, and J. K. Yungel, "Satellite retrieval of inherent optical properties by inversion of an oceanic radiance model: a preliminary algorithm," *Appl. Opt.* **38**, 495–504 (1999).
12. F. E. Hoge and P. E. Lyon, "Spectral parameters of inherent optical property models: feasibility of satellite retrieval by matrix inversion of an oceanic radiance model," *Appl. Opt.* **38**, 1657–1662 (1999).
13. F. E. Hoge and P. E. Lyon, "Satellite observation of chromophoric dissolved organic matter (CDOM) variability in the wake of hurricanes and typhoons," *Geophys. Res. Lett.* **29**, doi:10.1029/2002GL015114 (2002).

14. F. E. Hoge, C. W. Wright, P. E. Lyon, R. N. Swift, and J. K. Yungel, "Inherent optical properties imagery of the western North Atlantic Ocean: horizontal spatial variability of the upper mixed layer," *J. Geophys. Res.* **106C**, 31129–31138 (2001).
15. Z. P. Lee, K. L. Carder, J. Marra, R. G. Steward, and M. J. Perry, "Estimating primary production at depth from remote sensing," *Appl. Opt.* **35**, 463–474 (1996).
16. M. J. Behrenfeld, E. Maranon, D. Siegel, and S. B. Hooker, "Photoacclimation and nutrient-based model of light-saturated photosynthesis for quantifying oceanic primary production," *Mar. Ecol. Prog. Ser.* **228**, 103–117 (2002).